Chapter 2

Flow Cytometry for Hematopoietic Cells

Daniela S. Krause, Michelle E. DeLelys, and Frederic I. Preffer

Abstract

Within the last 25 years, flow cytometry and fluorescence-activated cell sorting have emerged as both routine diagnostic tools in clinical medicine and as advanced analytic tools critical in performing scientific research. This chapter aims at summarizing the use of flow cytometry in benign and malignant hematology and the monitoring of inherited and acquired immunodeficiency states. Numerous figures are provided from our laboratories at Massachusetts General Hospital that illustrate examples of these conditions. The chapter also describes novel flow cytometry-based imaging techniques, the combination of flow cytometry and mass spectrography, new software tools, and some future directions and applications of advanced instrumentation for flow cytometry.

Key words Flow cytometry, Diagnostic immunophenotyping, Hematopoietic malignancies, Hematopathology, Immunodeficiencies, Hematopoietic stem cells, Bone marrow transplantation, Paroxysmal nocturnal hemoglobinuria, Amnis imaging cytometry, CyTOF mass cytometry, Gemstone probability state model

1 Introduction

The fascination of humans by blood dates back to the ancient Greek physician Hippocrates (460–377 B.C.), who referred to blood (Greek: "haima") as one of the four humors besides black bile (Greek: "melan chole"), yellow bile (Greek: "chole"), and phlegm (Greek: "phlegma"). With the development of the first microscopes in the seventeenth century, the interest turned to the corpuscular elements of the blood and the first description of cells in cork by the English natural philosopher, scientist, and architect Robert Hooke. Via the "cell theory" proposed by Theodor Schwann, Matthias Jakob Schleiden, Rudolf Virchow, and others in the nineteenth century, we have now arrived in an age in which hematopoietic cells and their earliest precursor cells can be isolated by techniques such as flow cytometric cell sorting, analyzed on a molecular level, expanded in vitro, and used therapeutically for hematopoietic stem cell transplantation. Efforts are now even being made to generate hematopoietic stem cells from skin fibroblasts in

Meral Beksaç (ed.), *Bone Marrow and Stem Cell Transplantation*, Methods in Molecular Biology, vol. 1109,
DOI 10.1007/978-1-4614-9437-9_2,

the form of induced pluripotent stem cells. The easy availability of hematopoietic cells has been beneficial for these developments over the centuries.

Flow cytometric immunophenotyping has become an indispensable part of the clinical laboratory, as it allows enumeration of specific cell types in different disease settings. This immunophenotyping, in conjunction with cytogenetics, molecular studies, and morphological assessment, is an essential diagnostic tool in hematopathology. In this chapter we will primarily present a broad overview of such possible immunophenotypic uses of flow cytometry in the clinical diagnostic laboratory.

2 Enumeration of Different Cell Types in Different Clinical Settings

2.1 Assessment of CD34+ Hematopoietic Stem Cells for Bone Marrow Transplantation

CD34+ cells are pluripotent hematopoietic stem cells (HSC) that via multiple precursor cell types are able to differentiate into the lymphoid, myeloid, erythroid, and megakaryocytic lineages. HSC are able to reconstitute hematopoiesis in an individual who has received high-dose chemotherapy and/or radiation [1–4]. HSC are collected from healthy donors (allogeneic) or patients with hematological malignancies (autologous) after mobilization of HSC from the HSC niche in the bone marrow by granulocyte colony-stimulating factor (G-CSF) and/or the CXCR4-antagonist, plerixafor, apheresis, or direct harvesting from the bone marrow. CD34+ HSC are enumerated by flow cytometry in order to assess whether the amounts of HSCs which have been collected are sufficient for the patient's body weight, usually around that is generally around $2–5 \times 10^6$ cells/kg body weight. Accurate quantification of CD34+ HSC is critical, as they are often transfused into a myeloablated patient.

This test is performed using antibodies to CD34 and CD45 and quantitation has recently been automated utilizing a probability state model [5]. Red blood cells are lysed and acquisition of 100,000 total CD45+ cells or at least 100 CD34+ cells [6], in order to achieve statistical significance, and analysis are usually performed immediately. Viability of HSC may be determined by the nuclear dye 7-AAD, which is excluded in viable cells (Fig. 1).

2.2 Enumeration of Immune Cells in Acquired and Inherited States of Immunosuppression

Flow cytometry is a well-established and largely automated method for monitoring T-cell subsets in HIV infection or during immunosuppression with calcineurin inhibitors like tacrolimus. Peripheral blood leukocytes are stained with antibodies to CD3, CD8, CD45, and CD4 for T-cell-subset analysis and possibly CD16, CD56, and CD19 for a more comprehensive analysis of NK cells and B-lymphocytes. The test may be performed as a single-platform technology using an internal bead standard to obtain absolute

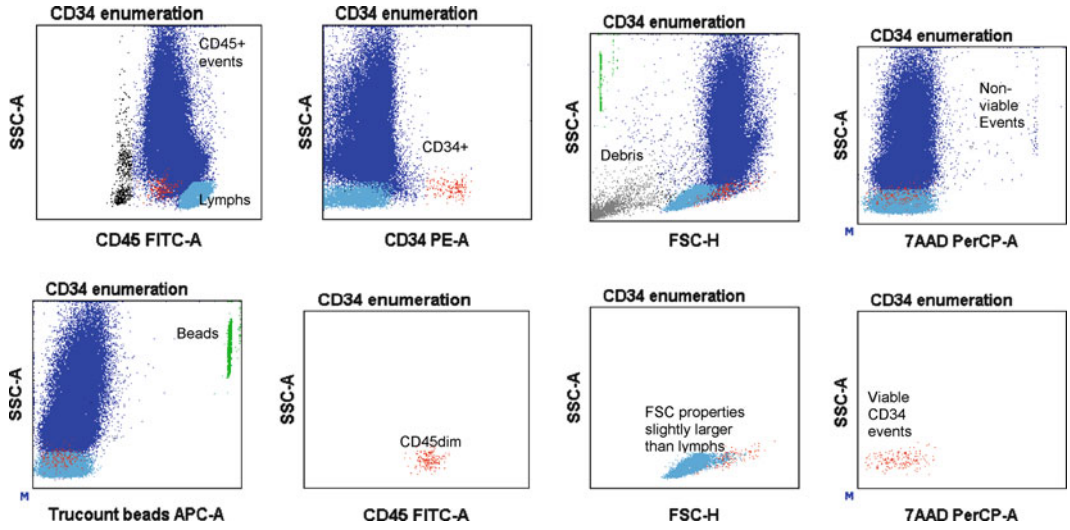

Fig. 1 Representative dot plots from a patient's apheresis product post bone marrow stem cell mobilization using the BD™ Stem Cell Enumeration Kit and the ISHAGE stem cell gating method [6]. The stem cells are gated sequentially first by gating on CD45+ events, next by gating on CD34+SSC^{low} events, and then by gating strictly on the CD45 dim events. Lastly it is ensured that the cells are similar in size (or slightly larger) to normal lymphocytes. The BD™ Stem Cell Enumeration Kit utilizes BD Trucount™ tubes, which allow for the determination of absolute numbers of stem cells as well as the viability dye 7AAD, to exclude nonviable events

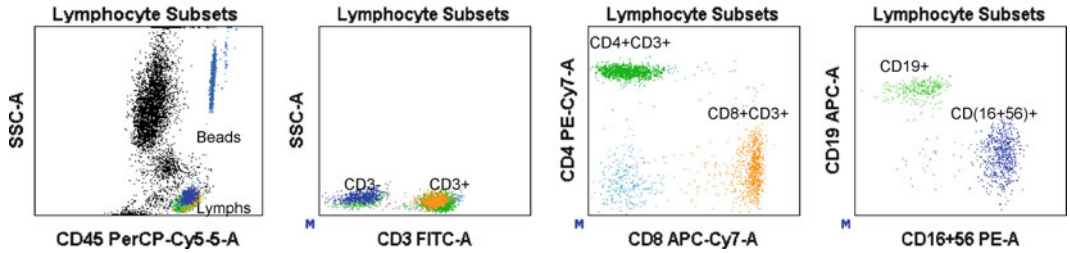

Fig. 2 Representative dot plots from a patient's peripheral blood to determine absolute counts of lymphocyte subsets using the BD Multitest™ TBNK kit. First lymphocytes are gated using CD45 and low SSC. T-cell subsets are determined as CD3+CD4+ and CD3+CD8+ events, NK cells are determined by gating on CD3– CD(16+56+) events, and B cells are determined by gating on CD3– CD19+ events. BD Trucount™ tubes allow for the accurate determination of absolute numbers of cells in non-piston delivery fluidic systems

counts of CD4+ and CD8+ T cells, obviating the need for a concomitant blood sample to obtain the patient's white blood cell count [7] (Fig. 2).

Common variable immune deficiency (CVID) is a group of inherited immune disorders characterized by decreased levels of most or all of the immunoglobulin subclasses; a decreased number of B cells and plasma cells, both involved in the production of antibodies; and an increased frequency of bacterial infections [8].

The genetic abnormalities associated with CVID vary greatly among patients and may involve the genes encoding CD19, the transmembrane activator and calcium-modulating cyclophilin ligand interactor (TACI), and others. Flow cytometry can aid in the diagnosis of CVID by investigation of the expression of CD27, IgM, and IgD on B cells. In contrast, severe combined immunodeficiency (SCID) is a more severe immune defect, as individuals with this disorder have defects in both B- and T-cell lineages. Babies born with this defect usually die of severe infections before the age of 1 year. Most forms of the disease are due to mutations in the gamma chain (γ_c) common to the receptor for several interleukins or due to a defect in adenosine deaminase (ADA). Flow cytometry may be helpful in analyzing expression of CD45RA versus CD45RO on T cells. In the autoimmune lymphoproliferative syndrome (ALPS), increased numbers of lymphocytes are found in lymph nodes, spleen, and liver leading to enlargement of these organs. ALPS can be associated with autoimmune disorders such as anemia, thrombocytopenia, and neutropenia. Aberrant T cells in this disease may be CD4– CD8– CD3+ TCRαβ+ B220+.

2.3 Monitoring of B Cells During Anti-B-Cell Immunosuppressive Treatment

An adequate response to the B-cell agent Rituxan (anti-CD20 therapeutic antibody) used for treatment of non-Hodgkin lymphoma and as immunosuppressant in several autoimmune disorders can be monitored by flow cytometry. The effects of Rituxan therapy are monitored by staining patient blood leukocytes with antibodies to CD45, CD19, and CD20 and observing the rapid and prolonged physical "clearance" of the B-cell lymphocyte subpopulation from the circulation (Fig. 3).

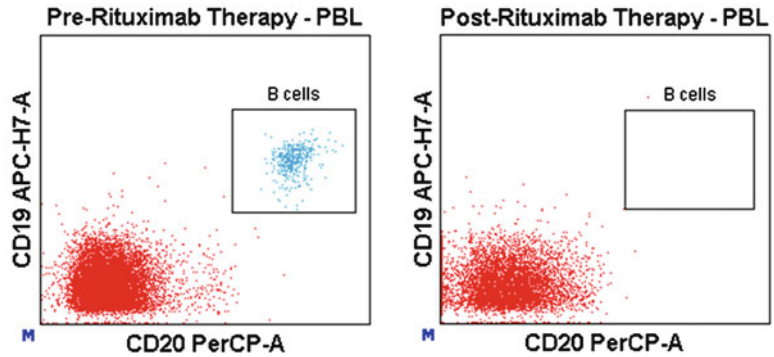

Fig. 3 Representative dot plots from a patient's peripheral blood pre-rituximab treatment (*left*) and post-rituximab treatment (*right*)

3 Diagnostic Use of Flow Cytometry in Hematological Malignancies

3.1 Leukemia

Flow cytometry is considered an integral part of determining the diagnosis of different types of leukemia and lymphoma. A pathological diagnosis is now made based on a combination of morphological, cytogenetic, and immunophenotypic criteria. When a leukemia is suspected, immunophenotypic analysis of leukocytes is usually performed on a whole blood or bone marrow aspirate anticoagulated with acid-citrate-dextrose (ACD) or ethylenediaminetetraacetic acid (EDTA). Other body fluids like CSF, ascites, or pleuritic fluid as mentioned in Subheading 3.5, however, can also be used. To determine the presence or absence of an unusual or a clonal population of T, B, NK, or myeloid cells that potentially represent a leukemia, in our laboratory a patient sample is stained in three separate tubes using the following eight directly conjugated monoclonal antibodies:

Tube 1: CD7, CD16, CD3, CD2, CD8, CD14, CD4, CD45

Tube 2: kappa, lambda, CD19, CD10, CD23, CD20, CD5, CD45

Tube 3: CD71, myeloperoxidase (MPO), CD34, CD33, CD117, HLA-DR, CD13, CD45

The antigens these monoclonal antibodies are directed against are located on the external surface membrane of the target cell. However, the MPO antigen is found within the cytoplasm, which thus requires permeabilization of the cell membrane for monoclonal antibody access. Acute myeloid leukemia (AML) cells are usually positive for permutations of CD13, CD33, CD34, CD117, and/or MPO and might variably express HLA-DR, CD56, and/or CD15 (Table 1) (Fig. 4). When lacking CD34 and CD117 and expressing CD14 or CD64, monocytic differentiation is likely; aberrant myelomonocytic, megakaryoblastic, erythroblastic, or basophilic differentiation may also be identified utilizing antibodies specific for these cell lineages. Myeloid malignancies might also confusingly co-express B- or T-lymphoid markers such as CD19, CD7, CD2, and/or CD5.

If acute promyelocytic leukemia is suspected (APML), CD64, CD11c, CD45, and CD11b can be used with $CD33^{bright}+$ as additional markers to try to identify this malignancy with its diagnostic t(15;17)(q22;q12) translocation and penchant to be associated with disseminated intravascular coagulation (DIC) (Fig. 5). HLA-DR, CD11b, CD11c, CD18, and CD34 are usually negative in APML. This disease responds very favorably to all-*trans*-retinoic acid therapy, which acts therapeutically to differentiate the tumor; rapid diagnosis of this disease is essential, to avoid DIC.

While flow cytometry is not routinely used yet on a widespread basis to diagnose myelodysplastic syndrome (MDS), staining for CD13, CD16, and CD11b on neutrophils as well as a variety of other markers on lymphocytes and stem cells of patients with

Table 1
Immunophenotype of selected hematological malignancies

Hematological malignancy	Common immunophenotypes
Acute myeloid leukemia	CD13+, CD33+, MPO+, CD117+, CD34+, HLA-DR+/–, CD14+/–, CD45^{dim}+
Acute promyelocytic leukemia	CD13+, CD33^{bright}+, MPO+, CD117+, CD34–, HLA-DR–, CD64+/–, CD11c+/–, CD45+/–, CD11b+/–
B-acute lymphoblastic leukemia/lymphoma	CD19+, CD20–, CD10+, TdT+, CD34+, CD45$^{dim\text{-}to\text{-}negative}$, absent light chain expression
Burkitt's lymphoma	CD19+, CD20+, CD10+, TdT–, CD23–, CD43+, CD5–, surface light chain restricted expression
Follicular lymphoma	CD19+, CD20+, CD10+, CD23+, CD43–, surface light chain restricted expression
Diffuse large B-cell lymphoma	CD19+, CD20+, CD10+, CD23+, CD5–, surface light chain restricted expression
Mantle cell lymphoma	CD19+, CD20+, CD10–, CD23–, CD43+, CD5+, FMC7+ surface light chain restricted expression
Chronic lymphocytic leukemia	CD19+, CD20^{dim}+, CD5+, CD23+, CD43+, FMC7–, surface light chain^{dim+} restricted expression
Hairy cell leukemia	CD19+, CD20^{bright}+, CD10–, CD5–, CD23–, CD103+, CD11c+, CD25+, surface light chain restricted expression
Marginal zone lymphoma	CD19+, CD20+, CD10–, CD23–, CD5–, CD43–, surface light chain restricted expression
Plasma cell myeloma	CD19–, CD38^{bright}+, CD138+, CD56+, CD45$^{dim+to\ neg}$ cytoplasmic light chain restricted expression
T-LGL	CD3+, CD2+, CD8+CD57+, CD56+, CD7+, CD16+, CD45+
T acute lymphoblastic leukemia/lymphoma	CD1a+, CD2+, CD3+, CD4+8+, CD5+, CD7+, TdT+; CD99+, CD34+, CD10+ (variably)
T-NHL	CD3+, CD7+, CD2+, CD4+ or CD8+
Cutaneous T-cell lymphoma	CD3+, CD2+, CD4+ and/or CD8+, CD5+/–, CD7+/– (CD26– in erythroderma)

suspected MDS may be employed. Flow cytometry, however, is widely being used to enumerate the percentage of blasts in MDS and for estimation of minimal residual disease in AML and B- and T-cell acute lymphoblastic leukemia (B-ALL and T-ALL, respectively). Multiple strategies to more directly assess MDS by flow cytometry are currently under investigation [9–14].

B-ALL cells frequently express CD19, CD10, nuclear terminal deoxynucleotidyl transferase (TdT), and cytoplasmic CD79a and/or CD22 (Fig. 6). CD34 and CD20 are variably expressed and

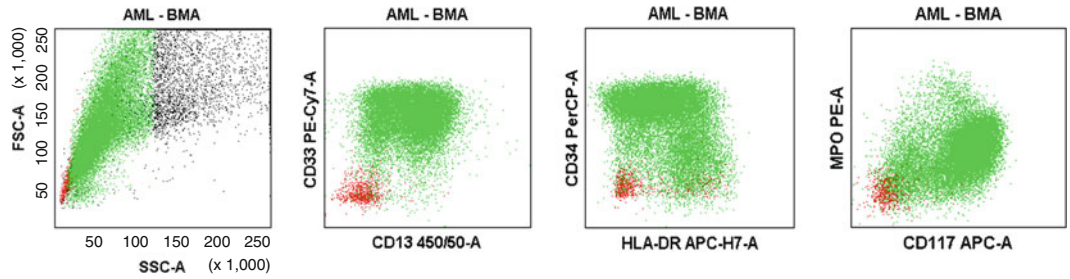

Fig. 4 Representative dot plots from a patient's bone marrow aspirate demonstrating acute myeloid leukemia (AML). The myeloid blasts are depicted as the green dots and express the characteristic immunophenotype of CD13+CD33+CD34+HLA-DR+MPO+CD117+. There is obvious variation in the expression of CD34, CD117, CD13, and HLA-DR demonstrated in this example, showing the heterogeneity of immunophenotypic expression. Myeloid blasts are larger than normal lymphocytes in size and have increased side scatter

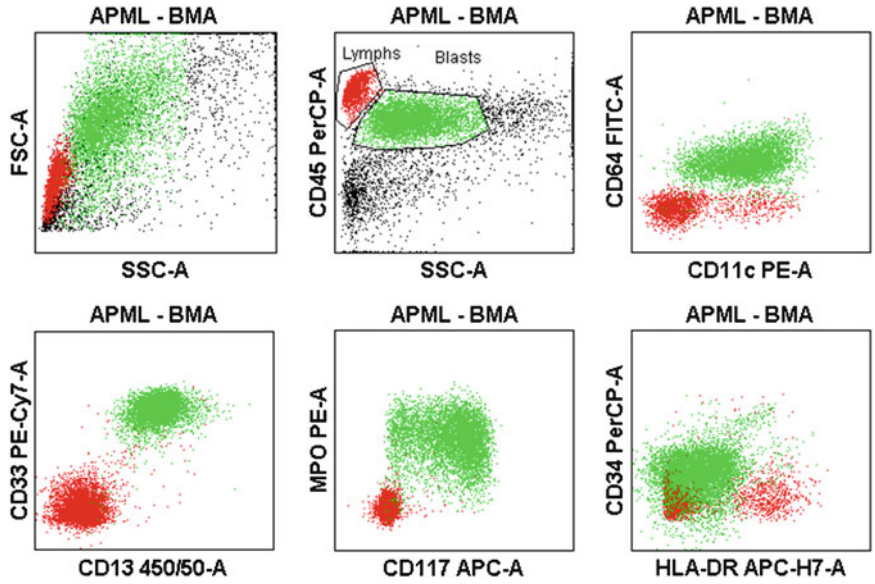

Fig. 5 Representative dot plots from a patient's bone marrow aspirate demonstrating acute promyelocytic leukemia (APML). The malignant promyelocytes are depicted as the *green dots* and express the characteristic immunophenotype of CD13+CD33^{bright}+CD64+CD11c+MPO+CD117+CD34–HLA-DR–. Promyelocytes have forward and side scatter characteristics similar to monocytes

CD45 is usually reduced from that appreciated on normal B cells or possibly entirely absent. Expression of the myeloid markers CD13 and/or CD33 is also possible and with cytoplasmic MPO expression would suggest a biphenotypic leukemia rather than diagnosis [15].

B cells in chronic lymphocytic leukemia (CLL) can immunophenotypically be described as CD19+, CD20^{dim}+, CD5+, and CD23+

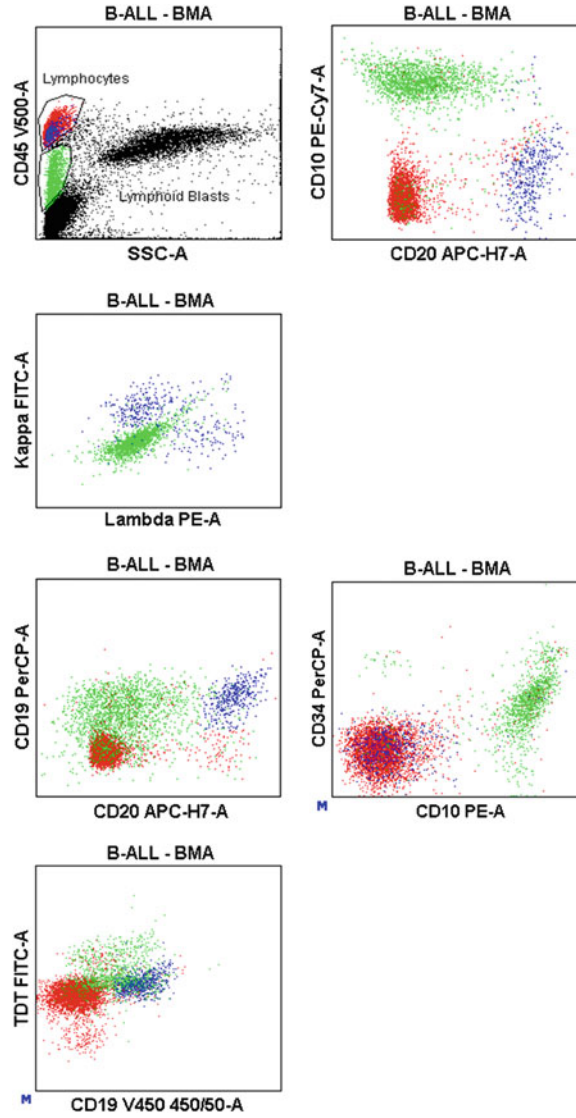

Fig. 6 Representative dot plots from a patient's bone marrow aspirate demonstrating B-cell acute lymphoblastic leukemia (B-ALL). The B-ALL cells are depicted as the *green dots* and the population of comingling normal B cells are depicted as the *blue dots*. B-ALL cells express the characteristic immunophenotype of CD19+ $CD20^{dim}$+CD10+CD34+TdT+$CD45^{dim/negative}$ without surface or cytoplasmic immunoglobulin light chain. B-ALL cells are typically somewhat larger than normal lymphocytes in size, but have similar side scatter properties

and are either kappa or lambda restricted (Fig. 7). The clonal immunoglobulin light chain expression is characteristically surface "dim" or actually only apparent in the cytoplasm after permeabilization. Hairy cell leukemia is positive for pan-B-cell markers and CD103, CD11c, and CD25 and usually negative for CD5, CD10,

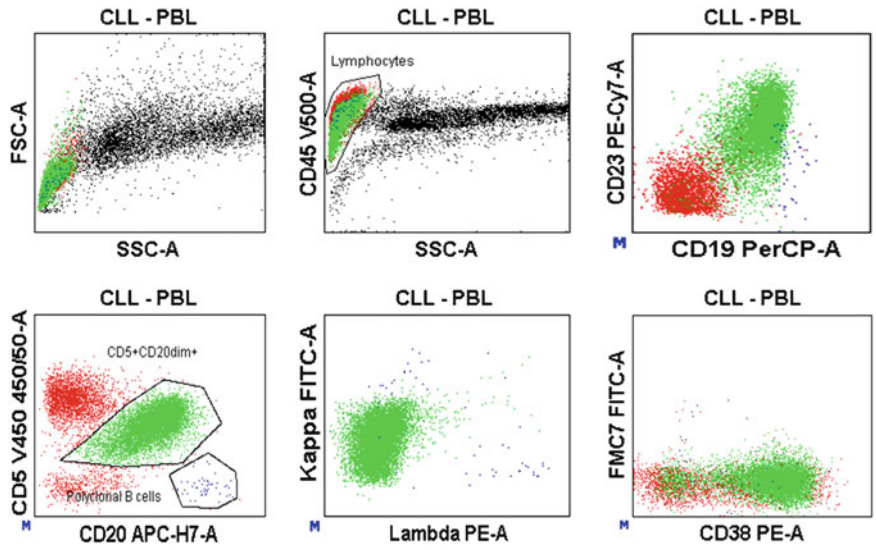

Fig. 7 Representative dot plots from a patient's peripheral blood demonstrating chronic lymphocytic leukemia (CLL). The CLL cells are depicted as the *green dots* and the population of comingling normal B cells are depicted as the *blue dots*. CLL cells express the characteristic immunophenotype of CD19+CD20^{dim}+CD5^{dim}+ CD23+CD38+/−FMC7−CD10− with reduced expression of monotypic light chain. Note the contrast of CD5, CD20, and light chain expression of these cells to those demonstrated in mantle cell lymphoma in Fig. 12. CLL cells have similar forward and side scatter properties to that of normal lymphocytes

and CD23; these tumor cells often have increased forward light scatter (Fig. 8). Antibody combinations used to detect large granular lymphocyte (LGL) leukemia include CD57, CD7, CD3, CD2, CD56, CD8, CD16, and CD45 (Fig. 9).

A new flow cytometric assay for the detection of the *BCR-ABL1* oncogene, causative of chronic myelogenous leukemia (CML), has been developed. With this methodology mononuclear cells are lysed and the *BCR-ABL1* fusion protein is bound by anti-BCR antibodies adsorbed to capture beads. Subsequently, a phycoerythrin-tagged anti-ABL1 antibody is used as the detector reagent to determine the mean fluorescence intensity. This assay reached 100 % concordance with the polymerase chain reaction method for reliable detection of the *BCR-ABL1* fusion protein [16], but its value for clinical diagnosis of CML will need to be assessed in the future. Flow cytometry, however, is well established as a reliable method to enumerate blast counts.

Leukemic stem cells (LSC) are rare leukemic cells which are resistant to chemotherapy and have acquired the ability to self-renew and induce disease in immunosuppressed mice upon xenotransplantation. As they are thought to reside in an LSC niche, from where they are hypothesized to give rise to relapsed disease, they have not been accessible for flow cytometry and their exact immunophenotype is uncertain. However, they are thought to

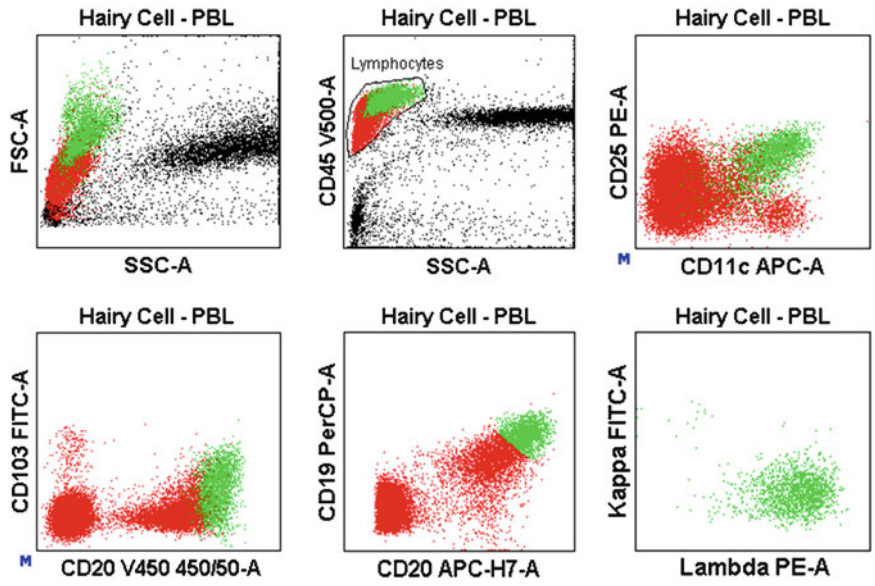

Fig. 8 Representative dot plots from a patient's peripheral blood demonstrating hairy cell leukemia. The "hairy cells" are depicted as the *green dots* and express the characteristic immunophenotype of CD19+CD20^{bright} +CD11c+CD25+CD103+ with monotypic light chain. Hairy cells are also larger than normal lymphocytes in size and have increased side scatter

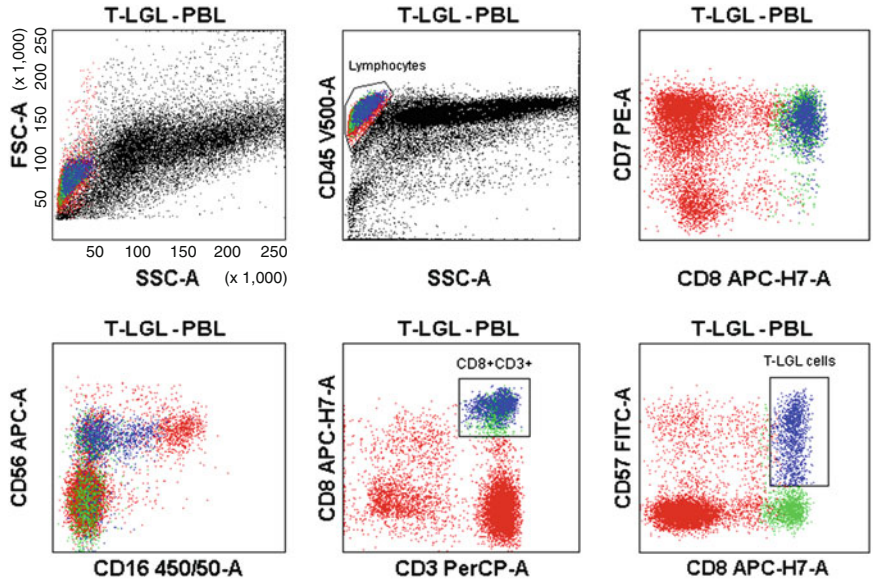

Fig. 9 Representative dot plots from a patient's peripheral blood with T-cell large granular lymphocytosis (T-LGL). The T-LGLs are depicted as the *blue dots* and immunophenotypically co-express CD3+CD8+ CD57+CD7+CD56+. This particular case does not express CD16. T-LGLs are typically slightly larger than normal lymphocytes in size and may have slightly increased side scatter

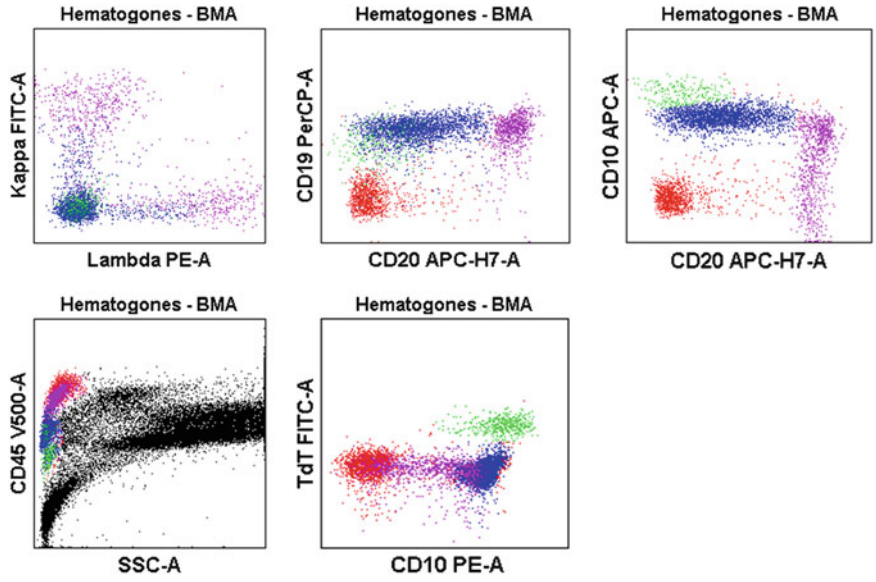

Fig. 10 Representative dot plots from a patient's bone marrow aspirate demonstrating normal B-cell maturation (hematogones). The least mature B-cell population is depicted as *green dots*, with the highest levels of CD10+ $CD19^{dim}$+CD20−$CD45^{dim}$+ lacking surface or cytoplasmic light chain expression and exhibiting very low side scatter. These also have nuclear TdT+ expression as well as elevated levels of CD38 and CD43 (not shown). The *blue dots* are in an intermediate state where the aforementioned markers are downregulated, while CD19, CD20, and surface immunoglobulin are upregulated. The *purple dots* represent the mature B-cell population. As the B cells undergo the maturation process, the immunophenotype ultimately progresses to TdT-CD10-CD19+CD20+CD45+ with either kappa or lambda surface light chain expression. *See* also Figs. 18 and 19

reside in the CD34+ CD38− fraction in AML [17, 18] and CML [19, 20] and in the CD34+ CD38− CD19+ fraction in B-ALL [21] (reviewed in ref. 4). Hematogones, benign lymphoid precursor cells, are frequently found in bone marrow aspirates, especially of young patients after chemotherapy (Figs. 10, 18, 19). They should not be confused with B-ALL blasts, as their immunophenotype (CD19+ CD20+ CD10+) is similar.

3.2 Lymphoma

Flow cytometry is used to immunophenotype lymphocytes in peripheral blood, fine needle aspirates, ascites, pleuritic fluid, or solid tissue specimens using T-, B-, and NK-cell markers, if a clonal population which may be consistent with a non-Hodgkin lymphoma (NHL) is suspected.

Our laboratory utilizes the following two tubes with eight conjugated monoclonal antibodies:

Tube 1: CD7, CD16, CD3, CD2, CD8, CD14, CD4, CD45

Tube 2: kappa, lambda, CD19, CD10, CD23, CD20, CD5, CD45

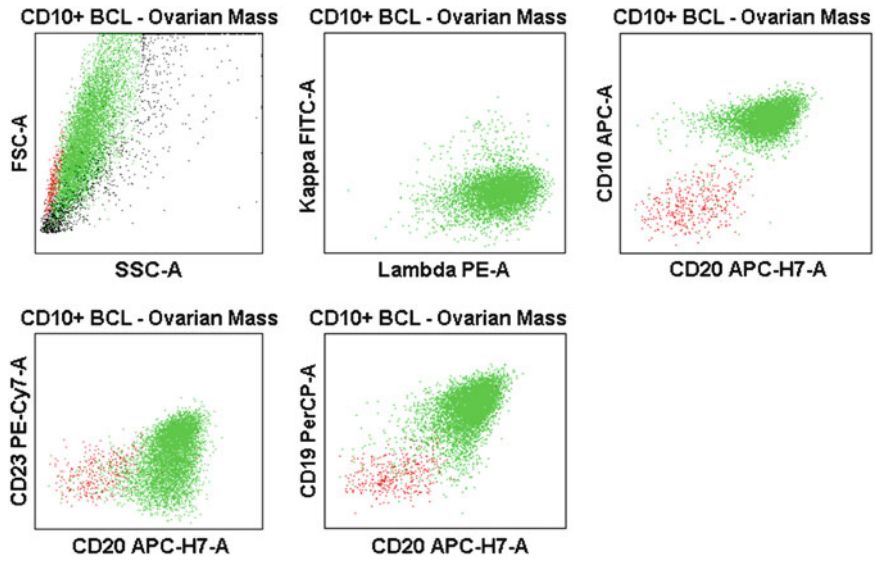

Fig. 11 Representative dot plots from a patient's ovarian mass demonstrating a CD10+ B-cell lymphoma (this patient was diagnosed with Burkitt's lymphoma based on the finding of the t(8;14) karyotype. However, this immunophenotype could also be consistent with follicular lymphoma). The Burkitt's cells are depicted as the *green dots* and express the characteristic immunophenotype of CD19+CD20+CD10+CD5−CD23+/− with monotypic lambda light chain. Burkitt's lymphoma cells are often larger than normal lymphocytes in size and have slightly increased side scatter

Follicular lymphoma (FL) is generally positive for CD19, CD10, CD23, CD20, and clonal kappa or lambda, while diffuse large B-cell lymphoma (DLBCL) frequently contains larger cells with an increased forward scatter and exhibits a similar immunophenotype: CD19, CD10, cytoplasmic CD79a, CD23, CD20, and clonal kappa or lambda, although light chain expression may be absent. Several cases of DLBCL overlap immunophenotypically with FL. However, some DLBCLs lack germinal center markers (as assessed by immunohistochemistry), so the immunophenotype can aid in excluding FL. However, cell size and pattern are very important in distinguishing between FL and DLBCL. In addition, DLBCL almost always has a higher proliferation index. Epstein–Barr virus or human herpes virus 8 may be detectable in some uncommon cases of DLBCL, while these are absent in FL. Burkitt's lymphoma is positive for CD19, CD20, and CD10 and further distinction from DLBCL and FL is achieved by histomorphology and immunohistochemical stains such as bcl-2 (Fig. 11). Similar to CLL, CD5-expression on B cells is frequently found in mantle cell lymphomas (MCL), but MCL is typically CD23– and FMC7+ and expresses CD20 and clonal kappa or lambda light chain more brightly than CLL [22] (Fig. 12). For suspected NHL in cerebrospinal or vitreous fluids, our laboratory uses the following

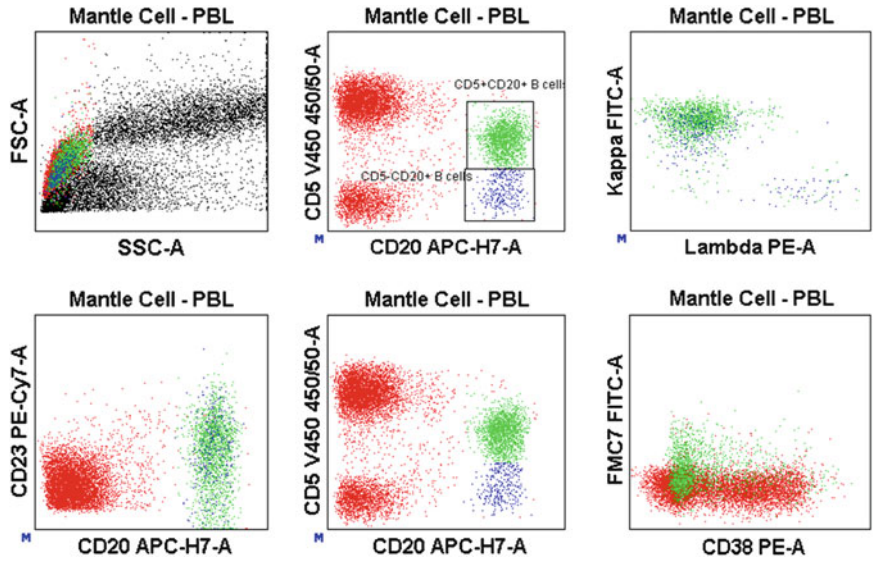

Fig. 12 Representative dot plots from a patient's peripheral blood demonstrating mantle cell lymphoma (MCL). The MCL cells are depicted as the *green dots* and the population of comingling normal B cells are depicted as the *blue dots*. MCL cells express the characteristic immunophenotype of CD19+CD20+CD5+CD23+/–CD3–FMC7+CD10– with monotypic light chain. In contrast to CLL, note that the tumor cells of mantle cell lymphoma are quite similar in their CD20 expression to the comingling normal B cells but that their restricted light chain expression is enhanced. MCL cells have similar forward and side scatter properties to that of normal lymphocytes

combination of directly conjugated antibodies: kappa, lambda, CD19, CD3, CD4, CD8, CD20, and CD45.

Common markers in T-NHL are CD3, CD7, CD2, CD4, and/or CD8. Clonal T-cell receptor rearrangements may be found by molecular diagnostic techniques. Sezary syndrome/mycosis fungoides/cutaneous T-cell lymphoma (CTCL) is positive for CD3, CD2, CD4, and/or CD8 (Fig. 13). Expression of CD5 and/or CD7 may be variable in CTCL and loss of CD26 is frequent in erythroderma associated with Sezary syndrome [23]. Although usually found in tissue sections and formerly not a good candidate for diagnostic testing by flow cytometry, Hodgkin's lymphoma can also be identified by flow-based immunofluorescence techniques [24].

3.3 Plasma Cell Myeloma

Plasma cell myeloma (PCM) is a malignancy of plasma cells. A plasma cell is a fully differentiated manifestation of a B cell that functions to produce antibodies. Malignant plasma cells usually express $CD38^{bright}$+, CD138+, CD19–, and $CD45^{dim}$+. They demonstrate monotypic expression of kappa or lambda light chains detected by cytoplasmic staining, and many additional markers are being investigated for their contribution to diagnosis, management, and detection of minimal residual disease (Fig. 14) [25–29].

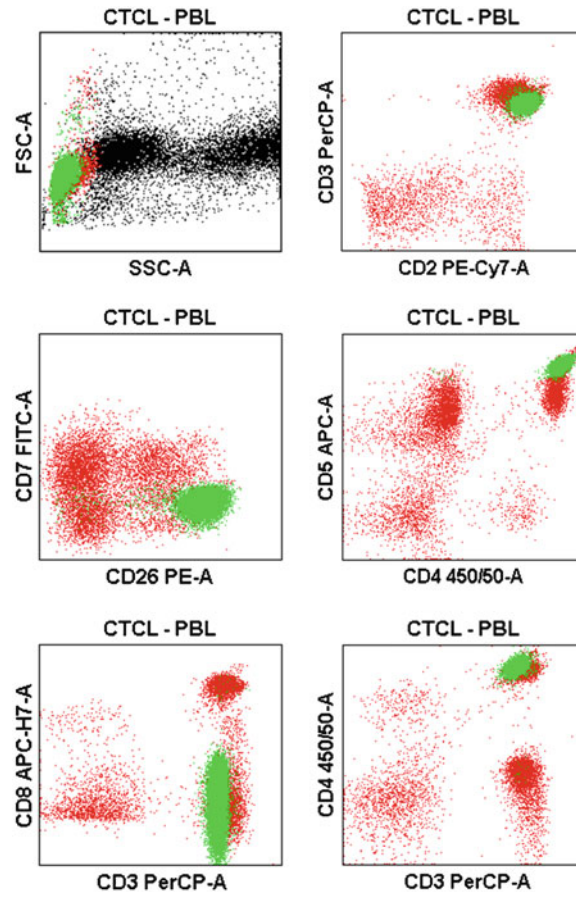

Fig. 13 Representative dot plots from a patient's peripheral blood demonstrating cutaneous T-cell lymphoma (CTCL). The CTCL cells are depicted as the *green dots* expressing the immunophenotype CD3+CD2+CD7−CD26+CD4+CD5^{bright}+ CD8−. However, CTCL immunophenotypes can be variable. CTCL cells have similar forward and side scatter properties to that of normal lymphocytes

3.4 The Use of Flow Cytometry in Other Diseases/Tissue Sites

3.4.1 Paroxysmal Nocturnal Hemoglobinuria

Paroxysmal nocturnal hemoglobinuria (PNH) is a rare acquired hematopoietic disorder caused by a mutation in the gene encoding for phosphatidylinositol glycan A (PIGA) [30, 31]. PIGA is a protein necessary for producing glycosylphosphatidylinositol (GPI), which anchors proteins to the cell membrane, in particular proteins which protect the cell from destruction by the complement system, like CD55 and CD59. Thus, patients with PNH have a complement-induced hemolytic anemia, hemoglobinuria, and thrombosis. Flow cytometry allows analysis of the expression of GPI-linked proteins on red blood cells (CD59), monocytes (CD14), and neutrophils (CD24), as well as the specific GPI-linked protein aerolysin identified by the fluorescently linked aerolysin (FLAER), expressed by peripheral blood lymphocytes; similar to CD34 quantitation

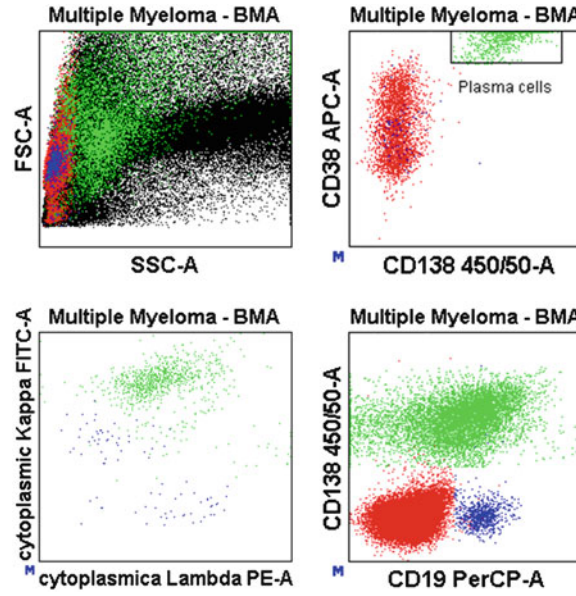

Fig. 14 Representative dot plots from a patient's bone marrow aspirate demonstrating plasma cell myeloma. The malignant plasma cells are depicted as the *green dots* and the population of comingling normal B cells are depicted as the *blue dots*. Plasma cells in plasma cell myeloma express the characteristic immunophenotype of CD138+CD38+CD19−/+CD45^{dim}+ with monotypic cytoplasmic light chain. Plasma cells are larger than normal lymphocytes in size and have slightly increased side scatter

described in Subheading 2.1, this type of analysis has also been automated with a new software approach utilizing a probability state model (Fig. 15) [32]. The reagent pallet and method of analysis continue to expand, with the improvement of the assay with CD64 as a marker for monocytes [33, 34]. The expression of these proteins is decreased or absent in patients with PNH. Staining with directly conjugated monoclonal antibodies is performed as follows:

Red blood cells (1:100 dilution): glycophorin, CD59

Monocytes (undiluted blood): FLAER, CD64, CD14, CD45

Neutrophils (undiluted blood): FLAER, CD24, CD15, CD45 [35]

In order to detect abnormal T-cell populations in patients infected with human T-cell lymphotropic virus (HTLV)-1, antibodies to CD25, CD7, CD3, CD2, CD5, CD8, CD4, and CD45 are used. Abnormal populations of eosinophils can be detected by staining for CD49d, CD33, CD294, and CD45.

Although a less sensitive test for the detection of giardia in stool samples than conventional microcopy or direct immunofluorescence, flow cytometry may be beneficial in detecting giardia cysts, particularly

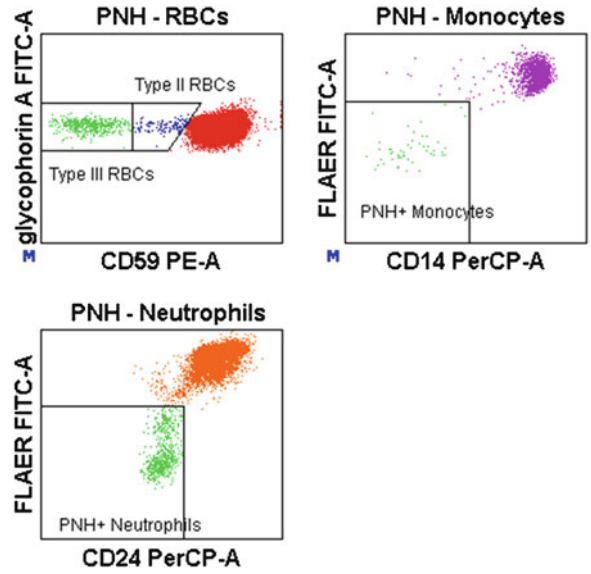

Fig. 15 Representative dot plots from a patient's peripheral blood demonstrating paroxysmal nocturnal hemoglobinuria (PNH). The events characterizing PNH can be seen in the red blood cell lineage (as CD59 dim-to-negative events), the monocytic lineage (as fluorescent aerolysin-/CD14– events), and the neutrophilic lineage (as fluorescent aerolysin-/CD24– events)

in epidemiological settings or in the absence of an experienced microscopist [36]. Furthermore, flow cytometry showed good correlation with the standard Kleihauer-Betke assay for the detection of fetomaternal hemorrhage with the use of an anti-hemoglobin F antibody [37]. Used in conjunction with other techniques, flow cytometry is also useful in the detection of malignancy by the analysis of paucicellular bronchoalveolar lavage (BAL) specimens [38] and GIST tumors [39] and the analysis of cerebrospinal fluid [40].

3.5 Recent Developments and the Near Future of Flow Cytometry

The field of flow cytometry continues to advance rapidly with exciting new developments. The technology may be thought of as a "three legged stool" that is supported by the synergy of hardware, software and fluorochrome biochemistry [41]. With respect to hardware, it has become obvious that high-resolution polychromatic flow cytometry (both for analysis and cell sorting) is greatly enhanced by both reducing the number of fluorochromes utilized per laser excitation beam and simultaneously increasing the number of excitation lines per instrument. This permits data production with little need for intra- or interlaser compensation and results in very clear concise data. This is presently far easier to do since the advent of extraordinarily small [relative to legacy water-cooled ion-gas lasers] fiber launched diode crystal lasers. With respect to these light sources, presently almost any line from the ultraviolet through

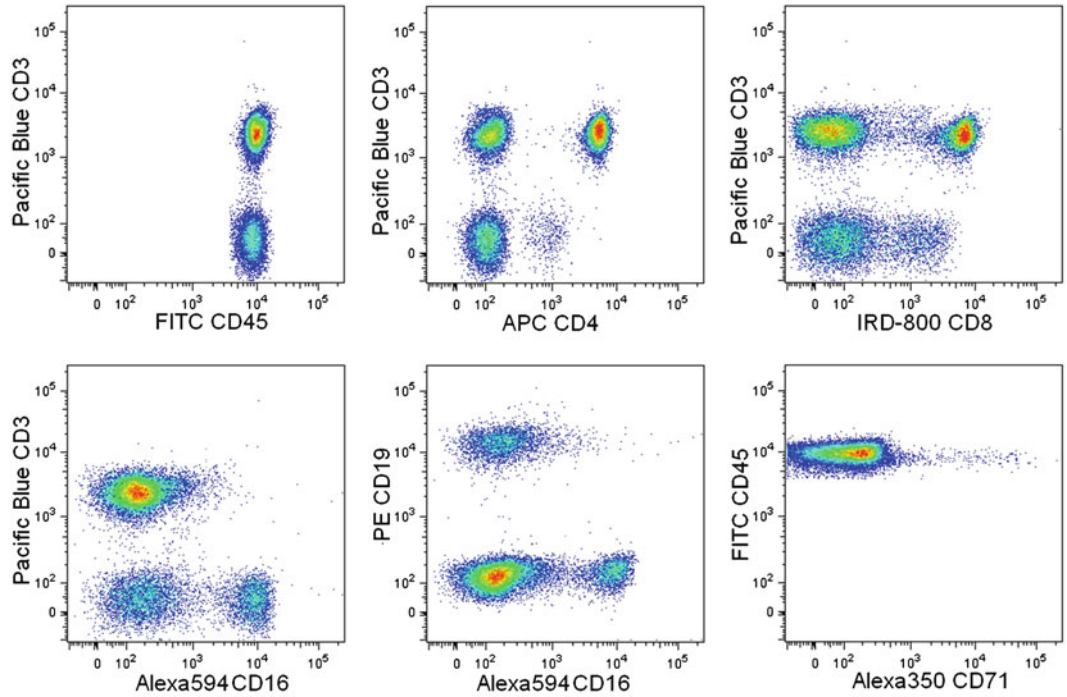

Fig. 16 Seven lasers for seven fluorochromes. Individual laser excitation of conjugated monoclonal antibodies demonstrates high resolution data. The following reagent-fluorochrome combinations were utilized and excited by the indicated laser line: CD71 Alexa 350 (355 nm), CD3 Pacific Blue (405 nm), CD45 FITC (488 nm), CD19 PE (532 nm), CD16 Alexa 594 (594 nm), CD4 APC (641 nm), and CD8 IRD 800 (785 nm). This results in virtually no fluorescence spillover and almost entirely obviates the need for intra- and interlaser compensation which when applied negatively impacts data resolution. The data was produced on the eight-laser platform depicted in Fig. 17

the infrared can be obtained from laser vendors and can be placed in a benchtop cytometer (Fig. 16). Filters now transmit light with almost 95 % efficiency, over relatively "flat" passbands, with sharp nanometer cutoff specifications (Fig. 17). Electronics in flow cytometers have recently been produced that surpass a 20-parameter limit, permitting up to 50 parameters to be monitored. Scalable software such as GemStone™ (Verity Software, Topsham ME) which is unrestricted regarding the number of parameters it can handle is available from a variety of sources (Fig. 18). Presently, the "bottleneck" in this tripartite paradigm is limitations in the organic-dye fluorochromes available. These dyes increase the spill-over between capture channels and require "compensation" which reduces data resolution. While not yet fully mature, it is hoped that increased flexibility in fluorochrome options will soon be forth-coming from companies such as Sirigen and their High Sensitivity Fluorescence™ technology that will not only expand the utility

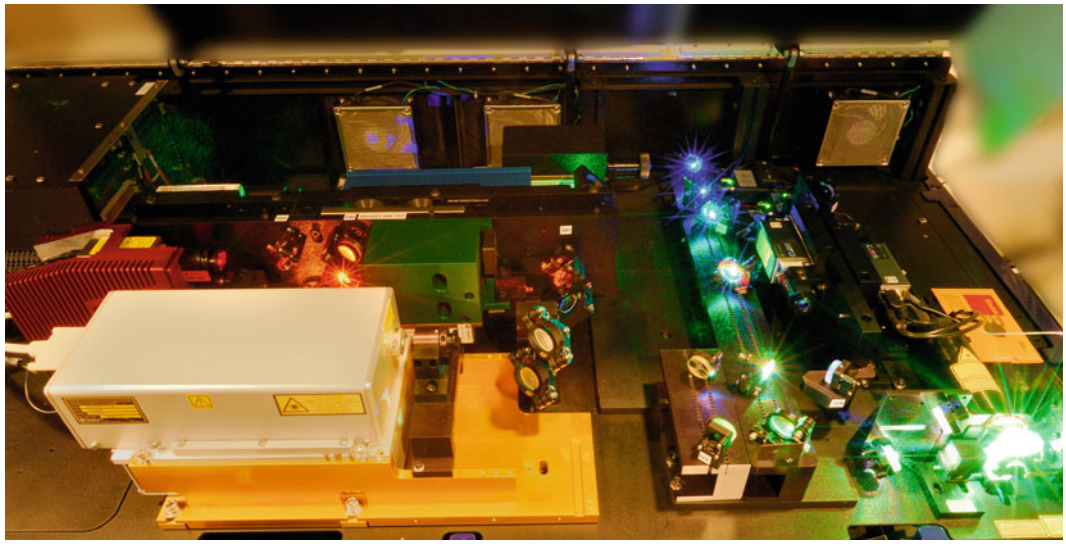

Wavelength	Power mw	Label
355	40	Coherent Genesis
405	100	Coherent Cube
488	100	Coherent Sapphire
532	150	Coherent Sapphire
552	100	Coherent Sapphire
594	200	MPB
641	100	Coherent Cube
785	40	Coherent Cube

Fig. 17 Eight-laser SORP LSR (Becton-Dickinson) flow cytometer. The benchtop flow cytometer depicted contains eight lasers with the indicated power characteristics. This provides highly flexible excitation capacity to the laboratory. When the appropriate fluorochromes are available, for the highest data resolution, it is best to reduce the numbers of fluorochromes excited per laser and increase the numbers of lasers used. Future versions of this platform will have the capacity to incorporate additional excitation lines and acquire up to 50 distinct parameters simultaneously

of the violet beam but lower energy beams further into the red spectrum as well.

Mass cytometry, utilizing the CyTOF™ platform (DVS Sciences, Sunnyvale CA), is another emerging technology that combines the analytical power of mass spectrometry with multiparameter flow cytometry. Antibodies or DNA intercalators are labeled with isotopes of transition elements and are mass analyzed and counted together with stained, vaporized, atomized, and subsequently ionized cell samples. Similar to immunofluorescence-based flow cytometry, the atomic ions and the tagging isotopes are counted in real time and can be analyzed on conventional flow cytometric software after having been converted to the FCS 3.0 format. With mass-tag cellular barcoding, mass cytometry throughput has been increased significantly, which will be invaluable for drug discovery, immunology,

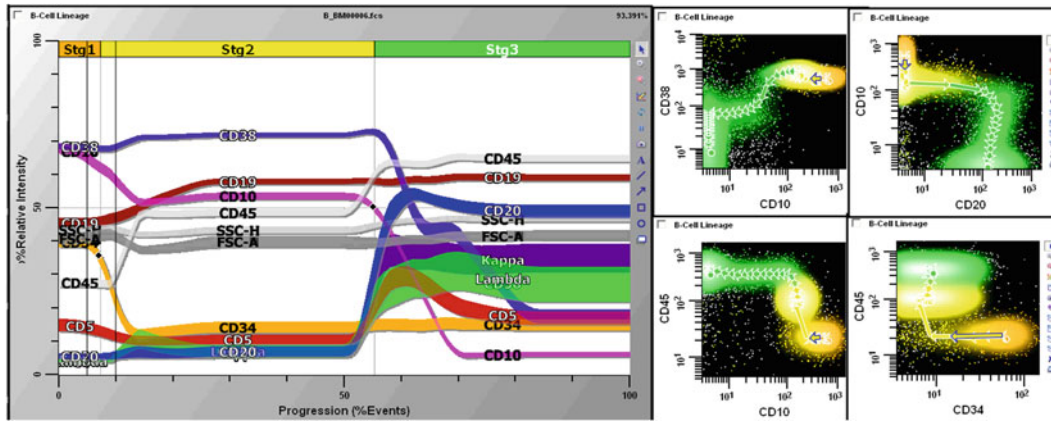

Fig. 18 This representation of normal human marrow B-cell maturation is depicted simultaneously both as a parameter profile plot (*left*) and four more conventional bivariate dot plots (*right*) by Gemstone™ Software (Verity Software House, Topsham, ME). B-cell maturation is initiated in human bone marrow by $CD19^{dim}$+ $CD45^{dim}$+ CD34+ CD38+ $CD10^{bright}$+ cells which downregulate CD10+, CD34+, and then CD38+ as they upregulate CD45, CD20, and surface immunoglobulin expression. While the dot-plot format shown is familiar to all flow cytometrists, interpreting high numbers of them becomes problematic for polychromatic analysis. The parameter profile plots are "scalable" and can display as many data points as the user wishes and are far more comprehensible to the non-cytometrist

preclinical analysis, and the understanding of the mechanisms of diseases and their treatments [42–45].

A breakthrough technology is found in the form of the Amnis instrument where flow cytometry can now be integrated with the power of visual microscopy. The Amnis platform fills an important gap in existing technology. While flow cytometry provides great statistical power, it provides relatively little information content per cell (results are based essentially on intensity only). On the other hand, fluorescence microscopy provides extremely high information per cell (as it is an image), but typically provides very poor statistical power.

The Amnis ISX platform couples important attributes of these two technologies on the same platform. The high acquisition rates obtained by "imaging in flow" enable the ability to utilize population statistics to assess differences in appearance rather than solely differences in fluorescence expression/intensity.

By leveraging the same basic fluidics (and fluorochrome excitation/emission) principles as traditional flow cytometry, statistically robust numbers of cells can be acquired for analysis on the Amnis platform. Unlike flow cytometry, images are taken of each cell in bright-field and fluorescent channels and intensity information is collected, enabling "statistical microscopy" to be performed on large populations of cells (Fig. 19).

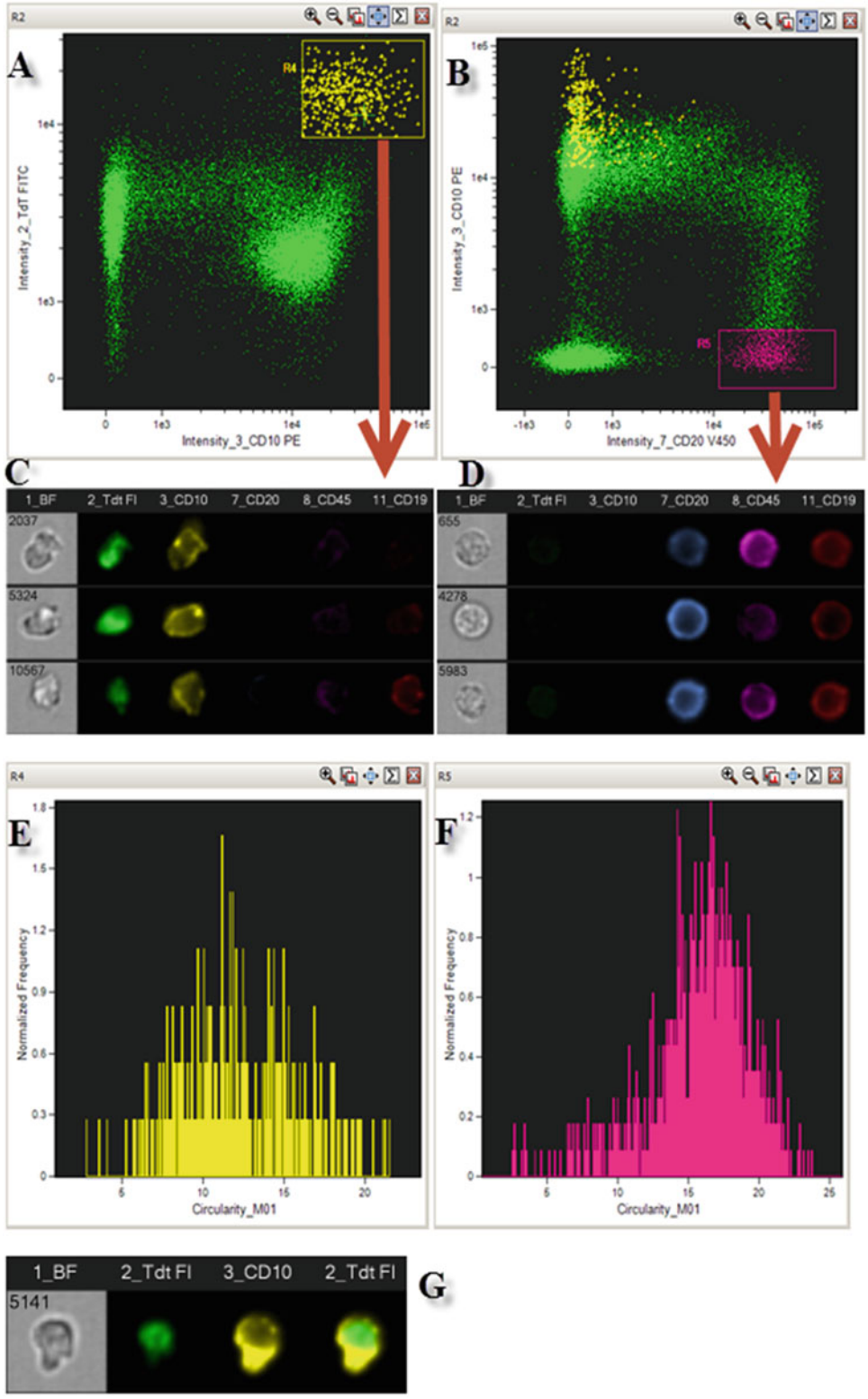

Fig. 19 Image-based flow cytometry. Specimens introduced into the Amnis ISX platform were initially assessed to be in focus (high gradient root mean square, in bright field), single cells (area vs. high aspect ratio, in bright field), and CD45+ with low side scatter characteristics. These human bone marrow cells were stained by standard techniques with TdT-FITC, CD10-PE, CD20-V450, CD19-APC, and CD45-V500. A bivariate dot plot (*panel a*) depicts TdT versus CD10 expression, with the brightest CD10+TdT+ cells identified in the R4 yellow gate.

Individual cells are captured on one to two cameras and can be displayed by both bright-field and fluorescence features. This capacity to localize the staining provides not only information on basic immunofluorescence but additionally the analysis of internalization and co-localization of proteins, cell death and autophagy, cell signaling, cell cycling, apoptosis, and DNA damage and repair. Furthermore, the imaging of cell-cell interactions and discrimination of cells from debris are also now far more accessible. These features are already being used in the research setting and could be exploited clinically in order to assess specific killing of a malignant cell in response to drug treatment, for example [46]. One exciting, novel clinical application of the Amnis instrument is rapid detection of intracellular promyelocytic leukemia (PML) protein in abnormal myeloid cells in patients with acute promyelocytic leukemia [47, 48]. In these patients, a rapid diagnosis is essential in order to initiate treatment with all-trans retinoic acid and cytostatic therapy, in order to prevent life-threatening coagulopathy, rapid disease progression, and death.

3.6 Summary

In summary, flow cytometry and its associated technologies are powerful aids in the evaluation and diagnosis of human disease states. Not only is flow cytometry helpful in the assessment and continuous monitoring of inherited or acquired immune disorders, but it is also invaluable in the monitoring of clinical response to various immunomodulatory therapies. This is in addition to the critical role it continues to play in basic and applied research. This is an exciting time in which our knowledge of human disease is rapidly growing, yet is becoming more and more complex, due to improved genome sequencing methods and technologies to understand epigenetic regulation of genes and finally personalized medicine. Flow cytometry and its more recent developments will, therefore, be instrumental in demonstrating to us the effects of genetic, epigenetic, and pharmacological alterations on a cellular, morphological, and more functional level.

Fig. 19 (continued) These cells are also shown to be CD20– in the CD10 versus CD20 plot (*panel b*). Each of the cells analyzed by the ISX is then individually assessed for their expression of each of the indicated markers and their bright-field image, as shown in the next row. For example, in *panel c*, the R4-gated CD10+TdT+ cells are seen to express nuclear TdT and bright membrane expression of CD10; there is only trace expression of CD20 and CD45 and CD19 is present, but this is relatively dimly expressed. The TdT+CD10^{bright}+CD19^{dim} +CD20– immunophenotype is characteristic of the least mature cells on the B-cell differentiation path in the bone marrow. In *panel d*, all the TdT and CD10 expression is downregulated, while the cells fully express CD45 and B-lineage associated CD19 and CD20. Completely novel and specific to ISX analysis is that the shape of the cells can be both visually inspected, and assessed statistically, and shown to be distinct; that is, the most mature B cells are seen to be "round" (bright-field column, *panel d*) compared to the least mature cells which are distinctly "not round" (bright-field column, *panel c*). This was enumerated and graphed on 1,143 and 361 cells, in *panels f* and *g*, respectively; the biological significance of this observation is not presently understood. Finally, the nuclear staining of TdT and CD10 membrane expression are overlaid in the last column of *panel g*

Acknowledgements

The authors would like to thank Laura Dillon, David Dombkowski, Abby Kelliher, and Scott Mordecai for their gracious help and specific contributions to this chapter.

Disclaimers

The authors have no conflicts of interest to disclaim.

Source of support: K08 CA138916-02 to DSK and grants 1S10OD012027-01A1 and 1S10RR020936-01 to FIP.

References

1. Spitzer TR, Dey BR, Chen YB, Attar E, Ballen KK (2012) The expanding frontier of hematopoietic cell transplantation. Cytometry B Clin Cytom 82:271–279
2. Preffer FI (2012) Issue highlights. Cytometry B Clin Cytom 82:343–344, November 2012
3. Rosko A, Lazarus HM (2012) Refining hematopoietic cell transplant: a concise review. Cytometry B Clin Cytom 82:266–267
4. Krause DS, Scadden DT, Preffer FI (2013) The hematopoietic stem cell niche—home for friend and foe? Cytometry B Clin Cytom 84: 7–20
5. Herbert DJ, Miller DT, Bruce Bagwell C (2012) Automated analysis of flow cytometric data for CD34+ stem cell enumeration using a probability state model. Cytometry B Clin Cytom 82:313–318
6. Whitby A, Whitby L, Fletcher M et al (2012) ISHAGE protocol: are we doing it correctly? Cytometry B Clin Cytom 82:9–17
7. Schnizlein-Bick CT, Spritzler J, Wilkening CL, Nicholson JKA, O'Gorman MRG (2000) Evaluation of TruCount absolute-count tubes for determining CD4 and CD8 cell numbers in human immunodeficiency virus-positive adults. Clin Diagn Lab Immunol 7:336–343
8. Warnatz K, Schlesier M (2008) Flow cytometric phenotyping of common variable immunodeficiency. Cytometry B Clin Cytom 74:261–271
9. van de Loosdrecht AA, Ireland R, Kern W et al (2013) Rationale for the clinical application of flow cytometry in patients with myelodysplastic syndromes: position paper of an International Consortium and the European LeukemiaNet Working Group. Leuk Lymphoma 54(3): 472–475
10. Bellos F, Alpermann T, Gouberman E et al (2012) Evaluation of flow cytometric assessment of myeloid nuclear differentiation antigen expression as a diagnostic marker for myelodysplastic syndromes in a series of 269 patients. Cytometry B Clin Cytom 82:295–304
11. Monaghan SA, Surti U, Doty K, Craig FE (2012) Altered neutrophil maturation patterns that limit identification of myelodysplastic syndromes. Cytometry B Clin Cytom 82:217–228
12. Della Porta MG, Lanza F, Del Vecchio L (2011) Flow cytometry immunophenotyping for the evaluation of bone marrow dysplasia. Cytometry B Clin Cytom 80:201–211
13. Kern W, Bacher U, Schnittger S, Alpermann T, Haferlach C, Haferlach T (2013) Multiparameter flow cytometry reveals myelodysplasia-related aberrant antigen expression in myelodysplastic/myeloproliferative neoplasms. Cytometry B Clin Cytom 84(3):194–197. doi:10.1002/cyto.b.21068
14. Sandes AF, Kerbauy DMB, Matarraz S, Chauffaille MD, López A, Orfao A, Yamamoto M (2013) Combined flow cytometric assessment of CD45, HLA-DR, CD34, and CD117 expression is a useful approach for reliable quantification of blast cells in myelodysplastic syndromes. Cytometry B Clin Cytom. doi:10.1002/cyto.b.21087
15. Swerdlow S, Campo E, Lee Harris N et al (2008) WHO classification of tumors of haematopoietic and lymphoid tissues, 4th edn. IARC, Lyon
16. Hevessy Z, Hudak R, Kiss-Sziraki V et al (2011) Laboratory evaluation of a flow cytometric BCR-ABL immunobead assay. Clin Chem Lab Med 50:689–692
17. Lapidot T, Sirard C, Vormoor J et al (1994) A cell initiating human acute myeloid leukaemia after transplantation into SCID mice. Nature 367:645–648

18. Bonnet D, Dick JE (1997) Human acute myeloid leukemia is organized as a hierarchy that originates from a primitive hematopoietic cell. Nat Med 3:730–737
19. Wang JCY, Lapidot T, Cashman JD et al (1998) High level engraftment of NOD/SCID mice by primitive normal and leukemic hematopoietic cells from patients with chronic myeloid leukemia in chronic phase. Blood 91: 2406–2414
20. Eisterer W, Jiang X, Christ O et al (2005) Different subsets of primary chronic myeloid leukemia stem cells engraft immunodeficient mice and produce a model of the human disease. Leukemia 19:435–441
21. Castor A, Nilsson L, Astrand-Grundstrom I et al (2005) Distinct patterns of hematopoietic stem cell involvement in acute lymphoblastic leukemia. Nat Med 11:630–637
22. Medd PG, Clark N, Leyden K et al (2011) A novel scoring system combining expression of CD23, CD20, and CD38 with platelet count predicts for the presence of the t(11;14) translocation of mantle cell lymphoma. Cytometry B Clin Cytom 80:230–237
23. Campbell SM, Peters SB, Zirwas MJ, Wong HK (2010) Immunophenotypic diagnosis of primary cutaneous lymphomas. J Clin Aesthet Dermatol 3:21–25
24. Fromm JR (2011) Flow cytometric analysis of CD123 is useful for immunophenotyping classical Hodgkin lymphoma. Cytometry B Clin Cytom 80:91–99
25. Cannizzo E, Bellio E, Sohani AR et al (2010) Multiparameter immunophenotyping by flow cytometry in multiple myeloma: the diagnostic utility of defining ranges of normal antigenic expression in comparison to histology. Cytometry B Clin Cytom 78:231–238
26. Paiva B, Almeida J, Pérez-Andrés M et al (2010) Utility of flow cytometry immunophenotyping in multiple myeloma and other clonal plasma cell-related disorders. Cytometry B Clin Cytom 78:239–252
27. Frébet E, Abraham J, Geneviève F et al (2011) A GEIL flow cytometry consensus proposal for quantification of plasma cells: application to differential diagnosis between MGUS and myeloma. Cytometry B Clin Cytom 80:176–185
28. Drain S, Catherwood MA, Bjourson AJ, Drake MB, Kettle PJ, Alexander HD (2012) Neither P-gp SNP variants, P-gp expression nor functional P-gp activity predicts MDR in a preliminary study of plasma cell myeloma. Cytometry B Clin Cytom 82:229–237
29. Peceliunas V, Janiulioniene A, Matuzeviciene R, Griskevicius L (2011) Six color flow cytometry detects plasma cells expressing aberrant immunophenotype in bone marrow of healthy donors. Cytometry B Clin Cytom 80:318–323
30. Sutherland DR, Keeney M, Illingworth A (2012) Practical guidelines for the high-sensitivity detection and monitoring of paroxysmal nocturnal hemoglobinuria clones by flow cytometry. Cytometry B Clin Cytom 82: 195–208
31. Marinov I, Kohoutova M, Tkacova V et al (2013) Intra- and interlaboratory variability of paroxysmal nocturnal hemoglobinuria testing by flow cytometry following the 2012 Practical Guidelines for high-sensitivity paroxysmal nocturnal hemoglobinuria testing. Cytometry B Clin Cytom 84(4):229–236
32. Miller DT, Hunsberger BC, Bagwell CB (2012) Automated analysis of GPI-deficient leukocyte flow cytometric data using GenStoneTM. Cytometry B Clin Cytom 82:319–324
33. Dalal BI, Khare NS (2013) Flow cytometric testing for paroxysmal nocturnal hemoglobinuria: CD64 is better for gating monocytes than CD33. Cytometry B Clin Cytom 84:33–36
34. Wong L, Davis BH (2013) Monochromatic gating method by flow cytometry for high purity monocyte analysis. Cytometry B Clin Cytom 84:119–124
35. Borowitz MJ, Craig FE, Digiuseppe JA et al (2010) Guidelines for the diagnosis and monitoring of paroxysmal nocturnal hemoglobinuria and related disorders by flow cytometry. Cytometry B Clin Cytom 78:211–230
36. El-Nahas HA, Salem DA, El-Henawy AA, El-Nimr HI, Abdel-Ghaffar HA, El-Meadawy HA (2013) Giardia diagnostic methods in human fecal samples: a comparative study. Cytometry B Clin Cytom 84:44–49
37. Pastoret C, Le Priol J, Fest T, Roussel M (2013) Evaluation of FMH QuikQuant for the detection and quantification of fetomaternal hemorrhage. Cytometry B Clin Cytom 84: 37–43
38. Song JY, Filie AC, Venzon D, Stetler-Stevenson M, Yuan CM (2012) Flow cytometry increases the sensitivity of detection of leukemia and lymphoma cells in bronchoalveolar lavage specimens. Cytometry B Clin Cytom 82: 305–312
39. Bozzi F, Conca E, Manenti G, Negri T et al (2011) High CD133 expression levels in gastrointestinal stromal tumors. Cytometry B Clin Cytom 80:238–247
40. Stacchini A, Demurtas A, Aliberti S (2012) Flow cytometric detection of liposomal cytarabine in cerebrospinal fluid of patients treated with intrathecal chemotherapy. Cytometry B Clin Cytom 82:280–282
41. Preffer FI, Dombkowski D (2009) Advances in complex multiparameter flow cytometry

technology: applications in stem cell research. Cytometry B Clin Cytom 76:295–314
42. Bodenmiller B, Zunder ER, Finck R et al (2012) Multiplexed mass cytometry profiling of cellular states perturbed by small-molecule regulators. Nat Biotechnol 30:858–867
43. Bandura DR, Baranov VI, Ornatsky OI et al (2009) Mass cytometry: technique for real time single cell multitarget immunoassay based on inductively coupled plasma time-of-flight mass spectrometry. Anal Chem 81:6813–6822
44. Bendall SC, Simonds EF, Qiu P et al (2010) Single-cell mass cytometry of differential immune and drug responses across a human hematopoietic continuum. Science 332:687–696
45. Wang L, Abbasi F, Ornatsky O et al (2012) Human CD4+ lymphocytes for antigen quantification: characterization using conventional flow cytometry and mass cytometry. Cytometry 81:567–575
46. Samsel L, Dagur P, Raghavachari N, Seamon C, Kato G, McCoy JP Jr (2013) Flow cytometry for morphologic and phenotypic characterization of rare circulating endothelial cells. Cytometry B Clin Cytom (in press). doi: 10.1002/cyto.b.21088
47. Grimwade L, Gudgin E, Bloxham D, Scott MA, Erber WN (2011) PML protein analysis using imaging flow cytometry. J Clin Pathol 64:447–450
48. Mirabelli P, Scalia G, Pascariello C et al (2012) ImageStream promyelocytic leukemia protein immunolocalization: in search of promyelocytic leukemia cells. Cytometry 81:232–237

http://www.springer.com/978-1-4614-9436-2

Bone Marrow and Stem Cell Transplantation
Beksaç, M. (Ed.)
2014, X, 313 p. 42 illus., 35 illus. in color., Hardcover
ISBN: 978-1-4614-9436-2
A product of Humana Press